

Collective modes of trapped Fermi gases with in-medium interaction

S.Chiacchiera,* T.Lepers,† and D.Davesne

Université de Lyon, F-69622 Lyon, France; Univ. Lyon 1, Villeurbanne; CNRS/IN2P3, UMR5822, IPNL

M.Urban

Institut de Physique Nucléaire, CNRS and Université Paris-Sud 11, 91406 Orsay Cedex, France

(Dated: December 1, 2008)

Due to Pauli blocking of intermediate states, the scattering matrix (or T matrix) of two fermionic atoms in a Fermi gas becomes different from that of two atoms in free space. This effect becomes particularly important near a Feshbach resonance, where the interaction in free space is very strong but becomes effectively suppressed in the medium. We calculate the in-medium T matrix in ladder approximation and study its effects on the properties of collective modes of a trapped gas in the normal-fluid phase. We introduce the in-medium interaction on both sides of the Boltzmann equation, namely in the calculation of the mean field and in the calculation of the collision rate. With mean field inclusion, we can considerably improve the agreement with measured temperature dependence of frequency and damping rate of the scissors mode. In addition, we compute frequencies and damping rates of the radial quadrupole and compression modes.

PACS numbers: 67.85.Lm

I. INTRODUCTION

In the last few years, experiments on collective modes in ultracold trapped Fermi gases at Duke University [1, 2] and at Innsbruck [3, 4, 5, 6] revealed a lot of interesting information about the different regimes which can be realized in these systems. This is mainly due to the possibility to change not only the temperature of the gas, but also the interaction between the atoms by adjusting the magnetic field in the vicinity of a Feshbach resonance. One of the objectives of these experiments was to detect the transition from the normal to the superfluid phase. However, although the frequencies of the collective modes are generally different in the hydrodynamic and in the collisionless regime, it was recognized that a hydrodynamic behaviour of the gas is not an unambiguous sign of superfluidity. In fact, hydrodynamic behavior can be a consequence of superfluidity, but also of a sufficiently high collision rate in the normal-fluid phase [7]. Recently it was therefore proposed to distinguish the superfluid, the collisionally hydrodynamic, and the collisionless regime [5].

The experimental results suggest that the transition from the superfluid to any of the normal-fluid regimes is always accompanied by a very strong damping of the collective modes. While the frequencies of the collective modes in the zero-temperature limit can easily be predicted in the framework of superfluid hydrodynamics, literature on the finite-temperature case is relatively sparse. One suggestion put forward by Griffin et al. was to apply Landau's two-fluid hydrodynamics [8], but this

requires that the collision rate in the normal-fluid component is sufficiently high, i.e., much higher than the mode frequency. This is usually not the case, since in a trapped system the collective modes have frequencies which are at least of the order of the trap frequency. In the opposite limit, i.e., if the normal-fluid component is collisionless, as it should be in the weakly interacting limit, a quasiparticle transport theory which couples superfluid hydrodynamics to a Vlasov equation for the normal component was suggested by one of the authors [9, 10, 11]. Although this theory provides a qualitative explanation of the damping of the collective modes near the transition from the superfluid to the collisionless normal-fluid phase, it cannot give a quantitative description of the recent experiments since these are generally done in the strongly interacting regime (near a Feshbach resonance).

In the normal phase, i.e., at temperatures above the critical temperature T_C of the superfluid-normal phase transition, the collective modes still exhibit a rather strong damping since the experiments are in fact neither in the collisionally hydrodynamic nor in the collisionless limit. This intermediate regime has been studied theoretically in the framework of the Boltzmann equation (sometimes also called Boltzmann-Vlasov or Landau-Vlasov equation). In the framework of the Boltzmann equation, interactions between the atoms enter in two different places: On the one hand, each particle moves in a mean field characterizing the average of the interaction with all other particles. On the other hand, the particles undergo two-body collisions, which are determined by the scattering cross-section.

In some of the early literature on this subject [12, 13, 14, 15, 16], the mean field effects were considered within the Hartree approximation. However, the most recent work by Bruun et al. [6, 17] concentrates mainly on the strongly interacting regime, where the Hartree approximation breaks down. While more and more sophisticated

*Present address: Centro de Física Computacional, Department of Physics, University of Coimbra, P-3004-516 Coimbra, Portugal

†Electronic address: t.lepers@ipnl.in2p3.fr

models of the collision term were developed, mean field effects were completely neglected. Therefore, the predicted frequencies in the collisionless limit are those of an ideal gas, and in the hydrodynamic limit, the equation of state is that of an ideal gas, too. However, at least the experiment of Ref. [4] clearly shows the importance of the mean field shift in the collisionless regime.

The aim of the present paper is to include mean field like effects on the propagation of the particles into the Boltzmann equation in a way which is appropriate for the strongly interacting case. Our approach is based on the in-medium scattering amplitude (T matrix), calculated in ladder approximation. This allows for a unified description of mean field like effects on the propagation of the particles (self-energy) and the modified cross-section entering the collision term of the Boltzmann equation. We point out that in order to have a consistent theory, it is important to use in the description of the collective modes, which are small variations around equilibrium, the same self-energy as in the calculation of the equilibrium density profile. This can be seen, e.g., by looking at the frequency of the sloshing mode, whose frequency, according to the Kohn theorem [18, 19], must be equal to the corresponding trap frequency.

Our paper is organized as follows. In Sec. II, we concentrate on the description of the strongly interacting Fermi gas in equilibrium. After illustrating the breakdown of the Hartree approximation, we review the treatment of the strongly interacting Fermi gas in the framework of the ladder approximation, introducing the in-medium scattering amplitude, the single-particle self-energy, and the in-medium cross-section. We discuss the quasiparticle approximation which is necessary for describing the system in the framework of the Boltzmann equation and which allows us to define a quantity similar to the mean field in Hartree approximation. We show the resulting density profiles and discuss the limits of validity of the quasiparticle approximation. In Sec. III, we turn to the description of collective modes in the framework of the Boltzmann equation, which now includes the “mean field” and the in-medium cross section. Using the standard method of taking moments of the Boltzmann equation in phase space, we obtain semi-analytic expressions for the collective mode frequencies which depend only on integrals of equilibrium quantities. In Sec. IV, we discuss our numerical results for the scissors, radial quadrupole, and breathing modes. Finally, in Sec. V, we draw our conclusions and give an outlook to further developments.

Throughout the paper, we will use in the derivations units with $\hbar = k_B = 1$ (\hbar = reduced Planck constant, k_B = Boltzmann constant).

II. IN-MEDIUM EFFECTIVE INTERACTION

A. Breakdown of the Hartree approximation

Let us consider a two-component (\uparrow, \downarrow) uniform Fermi gas in the normal phase. As long as the range of the interaction is small compared with the mean distance between atoms, one can assume a zero-range (δ function) interaction between atoms of opposite spin, and the hamiltonian reads (in second quantization)

$$H = \int d^3r \left(-\psi^\dagger \frac{\nabla^2}{2m} \psi + g \psi^\dagger_\downarrow \psi^\dagger_\uparrow \psi_\uparrow \psi_\downarrow \right), \quad (1)$$

where m and g denote the atom mass and the coupling constant and ψ is the fermion field operator. We assume that the interaction is attractive, i.e., $g < 0$. The coupling constant is related to the atom-atom scattering length a via

$$g = \frac{4\pi a}{m}. \quad (2)$$

In Hartree approximation, the single-particle energies of \uparrow and \downarrow particles are shifted by $U_{H\uparrow} = g\rho_\downarrow$ and $U_{H\downarrow} = g\rho_\uparrow$, respectively. The exchange or Fock term vanishes since the interaction is only between atoms with opposite spin. From now on, we will assume that both spin states are equally populated, and we denote by $\rho = \rho_\uparrow = \rho_\downarrow$ the density per spin state. Then the Hartree shift is the same for both spin states, and we may write

$$U_H = g\rho. \quad (3)$$

Let us now calculate the density as a function of the chemical potential μ . For our purposes it is enough to consider the zero-temperature limit, i.e., temperatures $T \ll \epsilon_F$, where

$$\epsilon_F = \frac{k_F^2}{2m} \quad \text{and} \quad k_F = (6\pi^2\rho)^{1/3} \quad (4)$$

are the Fermi energy and Fermi momentum, respectively. [Note that Eq. (4) defines ϵ_F and k_F for a uniform system, i.e., it remains valid even if the occupation numbers do not resemble a step function because of temperature or correlation effects. For a trapped system, however, we will use a different definition of ϵ_F and k_F , see Sec. II F.] At zero temperature, the relation between ϵ_F and μ is given by $\epsilon_F = \mu - U_H$. Substituting Eq. (3) into this relation, one obtains the following cubic equation for k_F :

$$-\frac{2ak_F^3}{3\pi m} - \frac{k_F^2}{2m} + \mu = 0. \quad (5)$$

It is easy to see that this equation does not have a solution if μ exceeds a critical value given by $\mu_{max} = \pi^2/(24ma^2)$, corresponding to a maximum density of $\rho_{max} = \pi/(48|a|^3)$. The same value was found in Ref. [20] as the density where the system becomes unstable

against separation into a low-density (gas) and a high-density (solid) phase.

If the above arguments were correct, a low-temperature Fermi gas with attractive interaction should be unstable as soon as $k_F|a| > \pi/2$. However, we know from experiments that ultracold Fermi gases are stable throughout the BCS-BEC crossover, including the unitary limit $k_F|a| \rightarrow \infty$, because the system prefers to form pairs instead of separating into two phases [21]. The instability is simply an artefact of the Hartree approximation and not physical.

B. T matrix

In the Hartree approximation as described in the previous subsection, the coupling constant g was related to the scattering length a in free space. This means that it was implicitly assumed that the scattering amplitude itself is the same in the gas as in free space. As we will see, this assumption is the origin of the unphysical instability of the Hartree approximation at high density or strong interaction. For instance, in Ref. [22] it was shown that the scattering amplitude becomes proportional to $1/k_F$ instead of a at high density.

The approximation scheme we adopt here in order to calculate the in-medium scattering amplitude is based on the non self-consistent T matrix approximation. In this approximation, the T matrix is given by the resummation of ladder diagrams, and it depends only on the total energy $E = \omega + 2\mu$ and the total momentum \mathbf{k} of the two atoms:

$$\Gamma(\omega, \mathbf{k}) = \frac{g}{1 - gJ(\omega, \mathbf{k})}, \quad (6)$$

where J denotes the non-interacting two-particle Green's function. Within the imaginary-time (Matsubara) formalism [23], the latter is given by

$$J(i\omega_N, \mathbf{k}) = -T \int \frac{d^3q}{(2\pi)^3} \sum_{n \text{ odd}} \mathcal{G}_0(\omega_n, \mathbf{k}/2 - \mathbf{q}) \times \mathcal{G}_0(\omega_N - \omega_n, \mathbf{k}/2 + \mathbf{q}), \quad (7)$$

where ω_N and ω_n are, respectively, bosonic and fermionic Matsubara frequencies, and $\mathcal{G}_0(\omega_n, \mathbf{k}) = 1/(i\omega_n - \xi_{\mathbf{k}}^0)$ is the free (Matsubara) Green's function, $\xi_{\mathbf{k}}^0 = k^2/(2m) - \mu$ being the free single-particle energy. After evaluation of the sum over n , the retarded function $J(\omega, \mathbf{k})$ is obtained as usual by analytic continuation. The result reads

$$J(\omega, \mathbf{k}) = \int \frac{d^3q}{(2\pi)^3} \frac{1 - n_{\mathbf{k}/2+\mathbf{q}}^0 - n_{\mathbf{k}/2-\mathbf{q}}^0}{\omega - \xi_{\mathbf{k}/2+\mathbf{q}}^0 - \xi_{\mathbf{k}/2-\mathbf{q}}^0 + i\eta}, \quad (8)$$

where $n_{\mathbf{k}}^0 = 1/[\exp(\beta\xi_{\mathbf{k}}^0) + 1]$, with $\beta = 1/T$.

The problem with Eqs. (6)–(8) is that J is divergent. To resolve this problem, one can introduce a momentum cut-off Λ , determine the coupling constant g as a function

of Λ such that one recovers the correct scattering length a in free space, and finally take the limit $\Lambda \rightarrow \infty$ keeping the free-space scattering length a constant [24]. In this way one obtains for the T matrix in free space

$$\Gamma_0(E, \mathbf{k}) = \frac{4\pi a}{m} \frac{1}{1 + iaq_{cm}}, \quad (9)$$

where $q_{cm} = \sqrt{mE - k^2/4}$ is the on-shell momentum in the center-of-mass (CM) frame. If we now decompose J into the two-particle Green's function in free space, J_0 , and a medium correction, \tilde{J} , such that $J = J_0 + \tilde{J}$, we may write

$$\Gamma(\omega, \mathbf{k}) = \frac{4\pi a}{m} \frac{1}{1 + iaq_{cm} - \frac{4\pi a}{m} \tilde{J}}, \quad (10)$$

with $q_{cm} = \sqrt{m(\omega + 2\mu) - k^2/4}$. Even without cut-off, the medium contribution \tilde{J} is finite and given by

$$\tilde{J}(\omega, \mathbf{k}) = - \int \frac{d^3q}{(2\pi)^3} \frac{n_{\mathbf{k}/2+\mathbf{q}}^0 + n_{\mathbf{k}/2-\mathbf{q}}^0}{\omega - \xi_{\mathbf{k}/2+\mathbf{q}}^0 - \xi_{\mathbf{k}/2-\mathbf{q}}^0 + i\eta}. \quad (11)$$

The imaginary part of \tilde{J} can be given in closed form:

$$\text{Im } \tilde{J}(\omega, \mathbf{k}) = \frac{m^2 T}{2\pi k} \ln \left(\frac{1 + e^{-\beta\xi_{\pm}^0}}{1 + e^{-\beta\xi_{\pm}^0}} \right), \quad (12)$$

where $\xi_{\pm}^0 = (k/2 \pm q_{cm})^2/(2m) - \mu$. The real part is then computed numerically via a dispersion relation,

$$\text{Re } \tilde{J}(\omega, \mathbf{k}) = -\mathcal{P} \int \frac{d\omega'}{\pi} \frac{\text{Im } \tilde{J}(\omega', \mathbf{k})}{\omega - \omega'}. \quad (13)$$

As a by-product, the in-medium T matrix allows us to determine the critical temperature T_C of the system, i.e., the temperature below which the system becomes superfluid. As realized by Nozières and Schmitt-Rink in their pioneering paper [21], the Thouless criterion which relates T_C to the temperature where the T matrix develops a pole at the Fermi level (i.e., at $\omega = 0$), remains true at all couplings. Since the pole always appears first at $\mathbf{k} = 0$, the critical temperature can be obtained from the equation

$$\text{Re } \tilde{J}(\omega = 0, \mathbf{k} = 0; T = T_C) = \frac{m}{4\pi a}. \quad (14)$$

C. Self-energy

Contrary to the zero-range interaction used in Sec. II A, the in-medium vertex function Γ is now momentum and energy dependent. This complicates the calculation of the single-particle energy shift. Even the concept of such an energy shift may be questioned if there are no well defined quasiparticles, as it is the case in the “pseudogap regime” [25]. In any case, the appropriate object to calculate is the single-particle self-energy Σ , which is

well-defined and does not rely on the existence of quasi-particles. The ladder self-energy can be written within the Matsubara formalism as

$$\Sigma(i\omega_n, \mathbf{k}) = \int \frac{d^3p}{(2\pi)^3} T \sum_{n' \text{ odd}} \mathcal{G}_0(\omega_{n'}, \mathbf{k}) \times \Gamma(i\omega_n + i\omega_{n'}, \mathbf{p} + \mathbf{k}). \quad (15)$$

Using analytic continuation to real energies, we find for the imaginary part of the retarded self-energy:

$$\text{Im} \Sigma(\omega, \mathbf{k}) = \int \frac{d^3p}{(2\pi)^3} \left(n_{\mathbf{p}}^0 + \frac{1}{e^{\beta(\omega + \xi_{\mathbf{p}}^0)} - 1} \right) \times \text{Im} \Gamma(\omega + \xi_{\mathbf{p}}^0, \mathbf{k} + \mathbf{p}), \quad (16)$$

which has to be evaluated numerically and from which the real part can be obtained by a dispersion relation analogous to Eq. (13).

Since we are going to use the Boltzmann equation for the description of collective modes, we are implicitly assuming that the quasi-particles, especially near the Fermi surface, are well defined, which is of course a limitation of the range of applicability of our approach [26]. If there are well-defined quasiparticles, this means that their dispersion relation $\xi_{\mathbf{k}}$, determined by the poles of the single-particle Green's function, can be obtained from

$$\xi_{\mathbf{k}} = \xi_{\mathbf{k}}^0 + \text{Re} \Sigma(\xi_{\mathbf{k}}, \mathbf{k}). \quad (17)$$

Such a treatment is probably desirable but beyond the scope of the present work. Here, we will completely neglect any energy and momentum dependence of the self-energy. Since we are mainly interested in momenta around the Fermi momentum, and hence energies around the Fermi energy, we will make the approximation

$$\xi_{\mathbf{k}} \simeq \xi_{\mathbf{k}}^0 + U, \quad \text{with} \quad U = \text{Re} \Sigma(0, k_{\mu}), \quad (18)$$

where $k_{\mu} = \sqrt{2m\mu}$ [which can actually be quite different from k_F as defined in Eq. (4)]. It is the quantity U which will take the role of the mean field potential in the Boltzmann equation.

D. Density

The fact that the particles are interacting among each other changes strongly the equation of state of the system, i.e., the relation between the chemical potential μ and the density ρ . Within the Hartree approximation, the relation $\rho(\mu)$ can trivially be obtained, whereas in ladder approximation, the calculation of the density for a given chemical potential μ is more involved.

In principle, the density can be obtained as

$$\rho = \int \frac{d^3p}{(2\pi)^3} T \sum_{n \text{ odd}} \mathcal{G}(\omega_n, \mathbf{p}) \quad (19)$$

where \mathcal{G} denotes the full single-particle Green's function, which according to Dyson's equation is given by $\mathcal{G}^{-1} = \mathcal{G}_0^{-1} - \Sigma$. Here we will restrict ourselves to an expansion of \mathcal{G} up to first order in Σ , i.e., we write

$$\mathcal{G} \simeq \mathcal{G}_0 + \mathcal{G}_0 \Sigma \mathcal{G}_0. \quad (20)$$

This leads us to the following expression for the density:

$$\rho = \rho_0 + \rho_1, \quad (21)$$

where the free (uncorrelated) part, ρ_0 , is given by

$$\rho_0 = \int \frac{d^3p}{(2\pi)^3} T \sum_{n \text{ odd}} \mathcal{G}_0(\omega_n, \mathbf{p}) = \int \frac{d^3p}{(2\pi)^3} n_{\mathbf{p}}^0, \quad (22)$$

while, after a lengthy calculation, the expression for the correlated part, ρ_1 , can be written as

$$\begin{aligned} \rho_1 &= \int \frac{d^3k}{(2\pi)^3} T \sum_{n \text{ odd}} \mathcal{G}_0^2(\omega_n, \mathbf{k}) \Sigma(i\omega_n, \mathbf{k}) \\ &= \int \frac{d^3k}{(2\pi)^3} \int \frac{d\omega}{2\pi} \frac{1}{e^{\beta\omega} - 1} \frac{d}{d\mu} \text{Im} \ln[-\Gamma(\omega, \mathbf{k})]. \end{aligned} \quad (23)$$

This is actually the result for the density initially given by Nozières and Schmitt-Rink (NSR) in Ref. [21] and by Sá de Melo, Randeria, and Engelbrecht [27].

Unfortunately, the density formula given above is not suitable for being used as the ground-state density in the Boltzmann equation. In the Boltzmann equation, the density is expressed as an integral over the distribution function f :

$$\rho = \int d^3p f(\mathbf{p}). \quad (24)$$

In the framework of the Boltzmann equation, the distribution function f must reduce to a simple Fermi function. Our quasiparticle(QP) approximation for the density consists in using the single-particle energy $\xi_{\mathbf{p}}$ as defined by Eq. (18) in the calculation of the occupation numbers, i.e.,

$$f_{eq}(\mathbf{p}) = \frac{1/A}{e^{\beta\xi_{\mathbf{p}}} + 1}, \quad (25)$$

where we have introduced the abbreviation $A = (2\pi)^3$. In this way we obtain an alternative method for calculating the density as a function of μ . Fortunately, it turns out that in most cases both ways of calculating the density give similar results. In order to demonstrate this, we show in Fig. 1 the dimensionless ratio μ/ϵ_F as a function of the parameter $1/(k_F a)$ defining the interaction strength for various temperatures (in units of the Fermi energy). One can see that the interactions lead to a reduction of μ with respect to the ideal gas result. At weak interactions, NSR and QP curves are in perfect agreement, but in the strongly interacting case there can be noticeable differences, especially at low temperatures close to T_C , indicating the breakdown of the QP approximation. This is not surprising, since in this case the system is in the ‘‘pseudogap regime’’ [25].

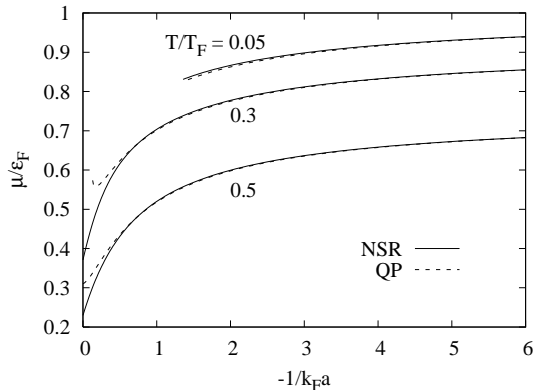


FIG. 1: The ratio μ/ϵ_F , with μ calculated with the NSR density and the QP density, is plotted as a function of $-1/k_F a$ for different temperatures: $T/T_F = 0.05$, $T/T_F = 0.3$ and $T/T_F = 0.5$. The curve for $T/T_F = 0.05$ stops at $1/k_F a \approx 1.36$, since at this interaction strength the critical temperature is reached.

E. Cross section

The interaction between atoms is not only responsible for the single-particle energy shift. It also determines the collision rate of the atoms, which will play a central role for the properties of collective modes. The important quantity is the cross section σ . In the case of a zero-range s -wave interaction, the cross section for two atoms in free space with momenta \mathbf{p}_1 and \mathbf{p}_2 before the collision and \mathbf{p}'_1 and \mathbf{p}'_2 after the collision is given by [16]

$$\frac{d\sigma_0}{d\Omega} = \frac{a^2}{1 + (qa)^2} \quad (26)$$

where $\mathbf{q} = (\mathbf{p}_1 - \mathbf{p}_2)/2$ is the incoming momentum in the CM frame and Ω is the solid angle after the scattering, i.e., $d\Omega = 2\pi \sin\theta d\theta$, where θ is the angle between \mathbf{q} and $\mathbf{q}' = (\mathbf{p}'_1 - \mathbf{p}'_2)/2$ (note that $|\mathbf{q}| = |\mathbf{q}'|$ because of energy and momentum conservation).

As pointed out in Refs. [6, 26], the cross section is strongly modified by medium effects. In terms of the T matrix, the in-medium cross section can be written as

$$\frac{d\sigma}{d\Omega} = \left| \frac{m}{4\pi} \Gamma \left(\frac{k^2}{4m} + \frac{q^2}{m} - 2\mu, \mathbf{k} \right) \right|^2 \quad (27)$$

which now depends also on the total momentum $\mathbf{k} = \mathbf{p}_1 + \mathbf{p}_2 = \mathbf{p}'_1 + \mathbf{p}'_2$ of the two atoms.

It is not easy to see a priori what will be the effect of these medium modifications, since depending on k and q the cross section can be enhanced or reduced as compared with the cross section in free space. This is shown in Fig. 2 where we display the cross section as a function of q for the case $k = 0$ (where the medium effect is supposed to be strongest) for various temperatures for fixed interaction strength $k_F a = -1$. The strong enhancement of the cross-section near the critical temperature is a precursor of the singularity of the T matrix at the critical temperature [6, 26].

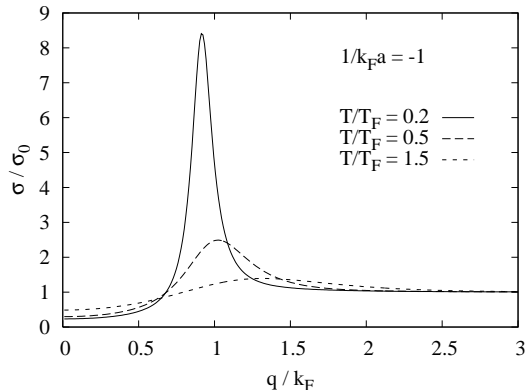


FIG. 2: The ratio of the in-medium cross section and the vacuum one is displayed for total momentum $k = 0$ as a function of the relative momentum q . The results are shown for different temperatures for fixed interaction strength $k_F a = -1$.

Let us mention that the same effect has already been found some years ago in the in-medium nucleon-nucleon cross section in low-temperature nuclear matter [28].

F. Local-density approximation

Until now we considered a uniform system where the atoms are not trapped by an external potential. In order to include the trap potential $V_T(\mathbf{r})$, we will make use of the local-density approximation (LDA), where the system is treated as locally homogeneous, with an \mathbf{r} dependent chemical potential which is given by

$$\mu(\mathbf{r}) = \mu_0 - V_T(\mathbf{r}). \quad (28)$$

This approximation should be valid as long as the potential varies only slowly, i.e., on length scales which are large compared with $1/k_F$. By the way, this condition is also necessary for the validity of the Boltzmann equation which will be used later to describe the collective modes.

Within the local-density approximation, all equilibrium quantities of the system discussed in the preceding sections, like Γ , U , ρ , $d\sigma/d\Omega$, etc., acquire an additional \mathbf{r} dependence via the dependence of μ on \mathbf{r} .

In practical calculations, we will use a harmonic trap potential

$$V_T(\mathbf{r}) = \frac{m}{2} \sum_{i=x,y,z} \omega_i^2 r_i^2. \quad (29)$$

Besides the fact that experimental traps are almost harmonic, the use of a harmonic potential has the advantage that it is sufficient to calculate the equilibrium quantities once for a spherical trap with the same number of atoms and the average frequency $\bar{\omega} = (\omega_x \omega_y \omega_z)^{1/3}$. Then, the equilibrium quantities in the deformed trap can easily be obtained from the corresponding ones in the spherical trap by the change of variables $\tilde{r}_i = r_i \omega_i / \bar{\omega}$ (for $i = x, y, z$).

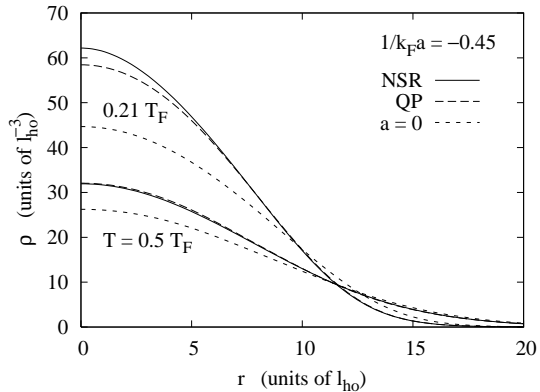


FIG. 3: Density profiles for 400000 atoms with $1/k_F a = -0.45$ at various temperatures, calculated using the NSR formula (solid lines) or the QP approximation (long dashes). For comparison, the corresponding density profiles of an ideal Fermi gas (short dashes) are shown, too. The length unit is the harmonic-oscillator length $l_{ho} = \sqrt{1/m\bar{\omega}}$.

As an example, we show in Fig. 3 the density profile of $N = 400000$ atoms in a trap with fixed interaction strength $1/k_F a = -0.45$ at different temperatures. Note that we follow here the usual convention of the experimental papers, using for the trapped gas a definition of k_F and ϵ_F which is different from that used in the uniform case [cf. Eq. (4)]. In the trapped case, k_F and ϵ_F refer to the values of k_F and ϵ_F in the center of the trap calculated for an *ideal* Fermi gas at *zero temperature*. Therefore, ϵ_F and k_F are determined by the number of atoms, N , and the average trap frequency as follows:

$$\epsilon_F = (3N)^{1/3}\bar{\omega}, \quad k_F = \sqrt{2m\epsilon_F}. \quad (30)$$

One can see that the interaction leads to a noticeable change of the density profile, especially at low temperature. The agreement between the NSR and QP results is almost perfect in the case $T/T_F = 0.5$, while at $T/T_F = 0.21$, corresponding to the critical temperature, the QP density is too small, indicating again the breakdown of the QP approximation in the pseudogap regime. However, it should be mentioned that for $1/k_F a = -0.45$, one has to go very close to T_C in order to see this effect; it is more important in the unitary limit. Let us mention that similar density profiles can be found in the literature, even for temperatures below the critical one [29].

III. COLLECTIVE MODES

A. Linearized Boltzmann equation

After the discussion of static properties, let us now turn to the description of collective modes of a trapped Fermi gas. We remind the reader of three assumptions mentioned earlier: (a) the density is supposed to vary (due to the trap as well as the collective motion) only on

large length scales; (b) the temperature has to be above the superfluid transition temperature T_C ; (c) the quasiparticles near the Fermi surface have to be well defined. In addition, the Boltzmann equation is only valid if (d) the time dependence of the excitations under consideration (in the case of the collective modes under consideration this time scale is set by the trap frequency) are slow compared to the “correlation time” [30]. Under these assumptions, the dynamics of the system can be described by the semi-classical distribution function $f(\mathbf{r}, \mathbf{p}, t)$ whose time evolution is governed by the Boltzmann equation [31]:

$$\dot{f} + \dot{\mathbf{r}} \cdot \nabla_{\mathbf{r}} f + \dot{\mathbf{p}} \cdot \nabla_{\mathbf{p}} f = -I[f], \quad (31)$$

where $\dot{\mathbf{r}}$ and $\dot{\mathbf{p}}$ satisfy the classical equations of motion. In the case of a quasiparticle dispersion relation as given by Eq. (18) with an \mathbf{r} dependent chemical potential as given by Eq. (28), the velocity and acceleration read

$$\dot{\mathbf{r}} = \nabla_{\mathbf{p}} \xi_{\mathbf{p}} = \frac{\mathbf{p}}{m}, \quad (32)$$

$$\dot{\mathbf{p}} = -\nabla_{\mathbf{r}} \xi_{\mathbf{p}} = -\nabla_{\mathbf{r}} (V_T + U), \quad (33)$$

since, within LDA, $\xi_{\mathbf{p}} \rightarrow \xi_{\mathbf{p}}(\mathbf{r}) = p^2/(2m) + V_T(\mathbf{r}) + U(\mathbf{r}) - \mu_0$. Note that there are two sources of \mathbf{r} dependence of the self-energy U . In equilibrium, U depends on \mathbf{r} only via $\mu(\mathbf{r}) = \mu_0 - V_T(\mathbf{r})$. More generally, in particular out of equilibrium, the self-energy depends on the distribution function f , i.e., we may write $U = U[f]$.

The distribution function f is related to the density per spin state by Eq. (24) and we assume that, as in equilibrium, the distribution functions for the two spin states are the same, i.e., $f_{\downarrow} = f_{\uparrow} = f$. This is true if the trap potential and the excitation operator of the collective mode are spin independent.

The functional $I[f]$ appearing on the rhs of Eq. (31) is the collision integral. It describes collisions between atoms with opposite spin and depends on the differential scattering cross section as [31]

$$I[f] = \int d^3 p_1 \int d\Omega \frac{d\sigma}{d\Omega} |\mathbf{v} - \mathbf{v}_1| [f f_1 (1 - A f') (1 - A f'_1) - f' f'_1 (1 - A f) (1 - A f_1)], \quad (34)$$

where \mathbf{p} and \mathbf{p}_1 are the incoming momenta, \mathbf{p}' and \mathbf{p}'_1 are the outgoing ones; \mathbf{v} and \mathbf{v}_1 are the incoming velocities \mathbf{p}/m and \mathbf{p}_1/m , respectively, Ω is the solid angle formed by the incoming relative momentum $\mathbf{p} - \mathbf{p}_1$ and the outgoing relative momentum $\mathbf{p}' - \mathbf{p}'_1$ of the two atoms, $f = f(\mathbf{r}, \mathbf{p}, t)$, $f_1 = f(\mathbf{r}, \mathbf{p}_1, t)$, $f' = f(\mathbf{r}, \mathbf{p}', t)$, etc. The factors of the type $(1 - A f)$ are absent in the classical Boltzmann equation. They are a consequence of Fermi statistics and ensure that an atom cannot be scattered into a state which is already occupied. This Pauli blocking effect can result in a strong reduction of the collision rate, especially at low temperatures.

In order to study the collective modes of the trapped gas, we consider a small deviation $\delta f = f - f_{eq}$ of the

distribution function from the equilibrium one. Usually δf is strongly peaked at the Fermi surface, but it can conveniently be written as

$$\delta f(\mathbf{r}, \mathbf{p}, t) = f_{eq}(\mathbf{r}, \mathbf{p})[1 - Af_{eq}(\mathbf{r}, \mathbf{p})]\Phi(\mathbf{r}, \mathbf{p}, t), \quad (35)$$

with a smooth function Φ [31]. Expanding the Boltzmann equation (31) to linear order in the deviations from equilibrium, and considering that a change δf of the distribution function results in a change δU of the self-energy, we obtain

$$f_{eq}(1 - Af_{eq})\left(\dot{\Phi} + \frac{\mathbf{p}}{m} \cdot \nabla_r \Phi - \nabla_r(V_T + U_{eq}) \cdot \nabla_p \Phi + \beta \frac{\mathbf{p}}{m} \cdot \nabla_r \delta U\right) = -I[\Phi] \quad (36)$$

with the linearized collision integral

$$I[\Phi] = \int d^3 p_1 \int d\Omega \frac{d\sigma}{d\Omega} |\mathbf{v} - \mathbf{v}_1| f_{eq} f_{eq1} \times (1 - Af'_{eq})(1 - Af'_{eq1})(\Phi + \Phi_1 - \Phi' - \Phi'_1). \quad (37)$$

Now we have to specify δU , which appears in the lhs of Eq. (36). Since we neglect any possible momentum dependence of U and δU , it is clear that δU can be written as

$$\delta U(\mathbf{r}, t) = \int d^3 p \gamma(p) \delta f(\mathbf{r}, \mathbf{p}, t), \quad (38)$$

where $\gamma(p)$ is the functional derivative $\delta U[f]/\delta f$, taken at f_{eq} . In the low-temperature limit, δf is so strongly peaked at the Fermi momentum p_F that $\gamma(p)$ may be replaced by a constant $\gamma_0 = \gamma(p_F)$, as in Fermi liquid theory [32]. This results in $\delta U = \gamma_0 \delta \rho$, with

$$\delta \rho(\mathbf{r}, t) = \int d^3 p \delta f(\mathbf{r}, \mathbf{p}, t) = \int d^3 p f_{eq}(1 - Af_{eq}) \Phi. \quad (39)$$

In addition, by choosing a particular form for δf , namely $\delta f = \partial f_{eq}/\partial \mu$, we can identify γ_0 with the derivative $\partial U_{eq}/\partial \rho_{eq}$ taken at constant T , i.e.,

$$\delta U(\mathbf{r}, t) = \left. \frac{\partial U_{eq}}{\partial \rho_{eq}} \right|_{\rho_{eq}(\mathbf{r}), T} \delta \rho(\mathbf{r}, t). \quad (40)$$

In the present work, we shall assume that Eq. (40) is a reasonable approximation also at higher temperatures, although it cannot be rigorously justified in this case.

Equation (36) together with (40) constitutes the starting point for our study of collective modes with in-medium effects. It is a generalization of the Boltzmann equation used in Refs. [13, 16] in the case $U = g\rho$ (Hartree approximation).

B. Trial function

As mentioned in Sec. III A, the function $\Phi(\mathbf{r}, \mathbf{p}, t)$ characterizing the deviation from equilibrium can be supposed to be smooth in phase space. This allows us to

make a simple ansatz for Φ with a small number of coefficients rather than solve the linearized Boltzmann equation (36) exactly.

For any collective mode of interest, the trial function $\Phi(\mathbf{r}, \mathbf{p}, t)$ has to contain at least those terms which are necessary to generate the velocity field $\mathbf{u}(\mathbf{r}, t)$ characterizing the mode [33]. The presence of a velocity field modifies f_{eq} into

$$f(\mathbf{r}, \mathbf{p}, t) = f_{eq}[\mathbf{r}, \mathbf{p} - m\mathbf{u}(\mathbf{r}, t)] \quad (41)$$

and leads to a deviation

$$\delta f \simeq -\beta f_{eq}(1 - Af_{eq}) \mathbf{p} \cdot \mathbf{u}, \quad (42)$$

i.e., the trial function Φ must at least contain a term proportional to $\mathbf{p} \cdot \mathbf{u}$. When this term is inserted into the linearized Boltzmann equation (36), the operator $\mathbf{p}/m \cdot \nabla_r - \nabla_r(V_T + U_{eq}) \cdot \nabla_p$ on the lhs of Eq. (36) generates new terms, as do the δU term on the lhs and the collision term I on the rhs. In general, the number of terms is infinite and the system cannot be closed.

However, in the case of an ideal gas ($U = \delta U = I = 0$) in a harmonic potential V_T , and if u is at most linear in the coordinates, it is possible to solve Eq. (36) with a finite number of terms. For instance, a term proportional to xp_x generates terms proportional to x^2 and p_x^2 , and no other terms are needed. In the opposite limit of an extremely strong collision term, i.e., in the hydrodynamic regime, a linear velocity field solves exactly the hydrodynamic equations if the equation of state can be approximated by a polytropic one, which is in many cases an excellent approximation [7]. We therefore assume that also in our case it will be a good approximation to include into Φ only those terms which appear in the ideal gas case (of course the coefficients will change).

To be explicit, we will focus on the scissors mode (S), the radial quadrupole mode (Q), and the breathing modes (B). In order to check the consistency of our model, we will also consider the Kohn mode (center-of-mass or sloshing mode, K). The velocity fields and the corresponding trial functions for these modes are given in Table I. Note that in the case of the breathing modes, we treat the axial and the radial mode together because they are coupled (although the coupling may be weak in very elongated traps).

C. Frequency and damping of collective modes

By inserting each trial function Φ into the linearized Boltzmann equation (36) and taking moments of the equation, namely multiplying it by any of the terms contained in Φ and then integrating over \mathbf{r} and \mathbf{p} , one obtains a set of homogeneous linear equations for the coefficients c_i . The condition that the coefficient matrix determinant is zero yields an equation for the frequencies of the collective mode.

TABLE I: Velocity fields and corresponding ansatz functions Φ for the different modes under consideration.

mode		trap frequencies	$\mathbf{u}(\mathbf{r}, t)$	$\Phi(\mathbf{r}, t)e^{i\omega t}$
sloshing	(K)	arbitrary	$\propto (1, 0, 0)$	$c_1x + c_2p_x$
scissors	(S)	$\omega_x > \omega_y \gg \omega_z$	$\propto (y, -x, 0)$	$c_1xy + c_2xp_y + c_3yp_x + c_4p_xp_y$
radial quadrupole	(Q)	$\omega_x = \omega_y = \omega_r \gg \omega_z$	$\propto (x, -y, 0)$	$c_1(x^2 - y^2) + c_2(xp_x - yp_y) + c_3(p_x^2 - p_y^2)$
radial } breathing	(B)	$\omega_x = \omega_y = \omega_r \gg \omega_z$	$\propto (x, y, 0)$	$\left\{ \begin{array}{l} c_1(x^2 + y^2) + c_2z^2 + c_3(xp_x + yp_y) \\ + c_4zp_z + c_5(p_x^2 + p_y^2) + c_6p_z^2 \end{array} \right.$
axial }			$\propto (0, 0, z)$	

Let us start by the center-of-mass oscillation of the cloud, known as sloshing or Kohn mode (K). In experiments, this mode is used in order to determine the trap frequency with high precision [4], since it is known to be an undamped oscillation with the frequency of the trap, independently of the interaction [18, 19]. It is an important test of the consistency of our method to check that this property is preserved.

Multiplying Eq. (36) (with $\Phi = c_1x + c_2p_x$) by x and p_x and integrating over \mathbf{r} and \mathbf{p} , we obtain the following system of equations [note that the collision term (37) on the rhs of the Boltzmann equation (36) does not contribute since $I[x] = I[p_x] = 0$]:

$$\frac{-i\omega}{m\omega_x^2} \left(N_\uparrow - \frac{C}{3} \right) c_1 - N_\uparrow c_2 = 0, \quad (43)$$

$$\left(N_\uparrow - \frac{C}{3} \right) c_1 - i\omega m N_\uparrow c_2 = 0, \quad (44)$$

where

$$N_\uparrow = \int d^3\tilde{r} \rho_{eq} \quad (45)$$

denotes the number of atoms per spin state and

$$C = \int d^3\tilde{r} d^3p \beta f_{eq} (1 - Af_{eq}) \tilde{r} \frac{\partial U_{eq}}{\partial \tilde{r}} \quad (46)$$

is a constant depending on the interaction. When calculating the determinant, we obtain $\omega = \omega_x$, independently of the interaction, as it should be. Of course, analogous results are obtained for the sloshing modes in the y and z direction.

If we repeat the same steps as before for the case of the scissors, quadrupole, or breathing mode, an additional complication arises from the fact that now the collision term on the rhs of the linearized Boltzmann equation (36) gives a non-vanishing contribution. More precisely, only the terms in Φ which are quadratic in momentum contribute, since $I[r_i r_j] = I[r_i p_j] = 0$ for $i, j = x, y, z$. Using the symmetry properties of the explicit expression for $I[p_i p_j]$, one can furthermore show that the $r_k r_l$ and $r_k p_l$ moments of $I[p_i p_j]$ ($i, j, k, l = x, y, z$) vanish and only moments involving two momenta,

$$I_{ijkl} = \int d^3r d^3p I[p_i p_j] p_k p_l, \quad (47)$$

survive. Using $I[p^2] = 0$, one can show that these must be of the form

$$I_{ijkl} = I_S \left(\delta_{ik} \delta_{jl} + \delta_{il} \delta_{jk} - \frac{2}{3} \delta_{ij} \delta_{kl} \right), \quad (48)$$

where I_S is the moment which is relevant for the scissors mode, i.e.,

$$I_S = I_{xyxy} = \int d^3r d^3p I[p_x p_y] p_x p_y. \quad (49)$$

Some more details on how I_S is calculated are given in Appendix B. Now let us define the corresponding relaxation time τ as

$$\frac{1}{\tau} = \frac{\int d^3r d^3p I[p_x p_y] p_x p_y}{\int d^3r d^3p f_{eq} (1 - Af_{eq}) p_x^2 p_y^2} = \frac{3\beta I_S}{m^2 E_{kin}}, \quad (50)$$

where E_{kin} denotes the kinetic energy (cf. Appendix A). It is essentially this parameter which governs the temperature dependence of the mode frequencies and damping rates. The definition (50) is identical with that introduced in Ref. [6].

Using the definition (50), we can write the equation for the scissors mode frequencies in the following form (see Appendix C for more details):

$$\frac{i\omega}{\tau} (\omega^2 - \omega_{S,h}^2) + (\omega^2 - \omega_{S,c+}^2) (\omega^2 - \omega_{S,c-}^2) = 0, \quad (51)$$

where $\omega_{S,h}$ and $\omega_{S,c\pm}$ are the frequencies in the hydrodynamic ($\omega\tau \rightarrow 0$) and collisionless ($\omega\tau \rightarrow \infty$) limits, respectively. The hydrodynamic frequency is given by

$$\omega_{S,h}^2 = \omega_x^2 + \omega_y^2, \quad (52)$$

and does not depend on the interaction. In the collisionless limit, there are two modes with different frequencies, corresponding to rotational [$\mathbf{u} \propto (y, -x, z)$] and irrotational [$\mathbf{u} \propto (y, x, 0)$] velocity fields. In a non-interacting gas, these two modes have the frequencies $\omega_{S,cl\pm} = \omega_x \pm \omega_y$. In the interacting case, they are changed to

$$\omega_{S,cl\pm}^2 = (\omega_x^2 + \omega_y^2) (1 - \chi/2) \pm \sqrt{4\omega_x^2 \omega_y^2 (1 - \chi + \chi^2/8) + (\omega_x^4 + \omega_y^4) \chi^2/4}, \quad (53)$$

where χ is the interaction dependent parameter defined in Eq. (A6).

For the radial quadrupole mode, the equation for the frequencies has the form

$$i\omega (\omega^2 - \omega_{Q,cl}^2) - \frac{1}{\tau} (\omega^2 - \omega_{Q,hd}^2) = 0, \quad (54)$$

the hydrodynamic frequency is, again, independent of the interaction and given by

$$\omega_{Q,hd}^2 = 2\omega_r^2, \quad (55)$$

while the frequency in the collisionless limit depends on the interaction:

$$\omega_{Q,cl}^2 = 4\omega_r^2(1 - \chi/2). \quad (56)$$

In the case $U = g\rho$ (Hartree approximation), χ reduces to $3E_{int}/2E_{pot}$, where E_{int} and E_{pot} denote the interaction and potential energies (cf. Appendix A). In this case, our limiting frequencies (in the hydrodynamic and collisionless limits: $\omega\tau \rightarrow 0$ and $\omega\tau \rightarrow \infty$) agree with those of Ref. [12, 16].

In the case of the breathing mode, we obtain two frequencies $\omega_{B\pm}$, corresponding to the axial and radial breathing modes. The low-lying mode (ω_{B-}) corresponds essentially to a motion in the z direction (axial breathing mode), while the high-lying mode (ω_{B+}) corresponds to a motion in the radial direction (radial breathing mode). The equation for the frequencies has the form

$$i\omega(\omega^2 - \omega_{B,cl+}^2)(\omega^2 - \omega_{B,cl-}^2) - \frac{1}{\tau}(\omega^2 - \omega_{B,hd+}^2)(\omega^2 - \omega_{B,hd-}^2) = 0. \quad (57)$$

The expressions for the limiting frequencies $\omega_{B,hd\pm}$ and $\omega_{B,cl\pm}$ are given in Appendix D.

IV. RESULTS AND DISCUSSION

In this section we will present our numerical results for the scissors, radial quadrupole, and radial breathing modes. We will discuss the frequencies and damping rates as functions of the temperature for finite values of $1/k_F a$ and for the unitary limit ($1/k_F a = 0$). The frequencies ω and damping rates Γ are determined by the real and imaginary parts of the solutions of Eqs. (51), (54), and (57), respectively.

So far, most experiments have been done on resonance, i.e., for $1/k_F a = 0$. Two exceptions are the study of the radial quadrupole mode over the whole crossover region by Altmeyer et al. [4] and of the scissors mode at $1/k_F a = -0.45$ by Wright et al. [5]. In addition to these two experiments, we will compare our results to the scissors, quadrupole, and breathing mode experiments at unitarity described in Refs. [5, 6].

A. Radial quadrupole mode at $1/k_F a = -1.34$

In the first experiment on the radial quadrupole mode on the BCS side of the BEC-BCS crossover [4], the trap had frequencies $\omega_r = 2\pi \times 370$ Hz and $\omega_z = 2\pi \times 22$ Hz

and contained $N = 400000$ ^6Li atoms. The highest magnetic field used in this experiment, corresponding to the weakest interaction, resulted in $1/k_F a = -1.34$, which is the value we will consider here. The temperature is unfortunately not known, but we assume that it was between $0.03T_F$, the lowest value ever reported by the Innsbruck group [34], and $0.1T_F$, the upper value given in Ref. [4].

Results for frequency and damping as functions of temperature are shown in the first two panels of Fig. 4, while the third panel shows the damping rate vs. the frequency. This latter representation was proposed in Ref. [6] in order to get rid of the temperature, which cannot easily be experimentally determined. The single data point shows unambiguously the necessity of the inclusion of the mean field since the measured frequency ($\sim 2.1\omega_r$) lies clearly above the limiting value for a collisionless gas without mean field ($2\omega_r$).

The theoretical curves shown in Fig. 4 represent different levels of approximation in the calculation. In order to see the effect of the different improvements of the theory, we include them one after another. We start with a classical Fermi gas (dotted lines), using Boltzmann distribution functions ($f_{eq} = e^{-\beta(p^2/2m+V_T-\mu_0)}$) in the calculation of the density profile, without any mean field effects and with the free cross-section, Eq. (26), without Pauli-blocking factors ($1 - Af_{eq}$) in the collision term. Within this approximation, the system shows hydrodynamic behavior ($\omega \rightarrow \sqrt{2}\omega_r$) at low temperature and collisionless behavior ($\omega \rightarrow 2\omega_r$) at high temperature, with strong damping Γ in the intermediate regime. In the representation of Γ vs. ω , this results in a curve similar to a semi-circle. The hydrodynamic behavior at low temperature is of course an artefact of neglecting the Pauli blocking in the collision term and it is in clear contradiction to the measured frequency.

In order to cure this problem, we include the effect of Fermi statistics (short dashes), i.e., we use the Fermi distribution function $f_{eq} = 1/(e^{\beta(p^2/2m+V_T-\mu_0)} + 1)$ in the calculation of the density profile, and the Pauli-blocking factors ($1 - Af_{eq}$) in the collision term. At this stage, we still use the free cross section and we do not include any mean field. Due to the Pauli blocking factors, the collision rate goes now to zero at low temperature, and therefore the system approaches the collisionless frequency $2\omega_r$ in both the low- and high temperature limits. The highest damping, and as a consequence the lowest frequency, is reached at a temperature of $\sim 0.3T_F$. Since no mean field is included, ω and Γ depend only on a single parameter, namely on τ [cf. Eq. (54)]. Therefore the results lie on the same curve in the $\omega - \Gamma$ plane as in the case of a classical gas (dotted curve), but this time only the small part of the curve corresponding to large values of τ is covered. Although the frequency at low-temperature is now in better agreement with the data, it is still too low, since we have not yet included the mean field.

The third step consists in switching on the mean field U (long dashes), i.e., the density profiles are now calculated with $f_{eq} = 1/(e^{\beta(p^2/2m+V_T+U-\mu_0)} + 1)$ and the

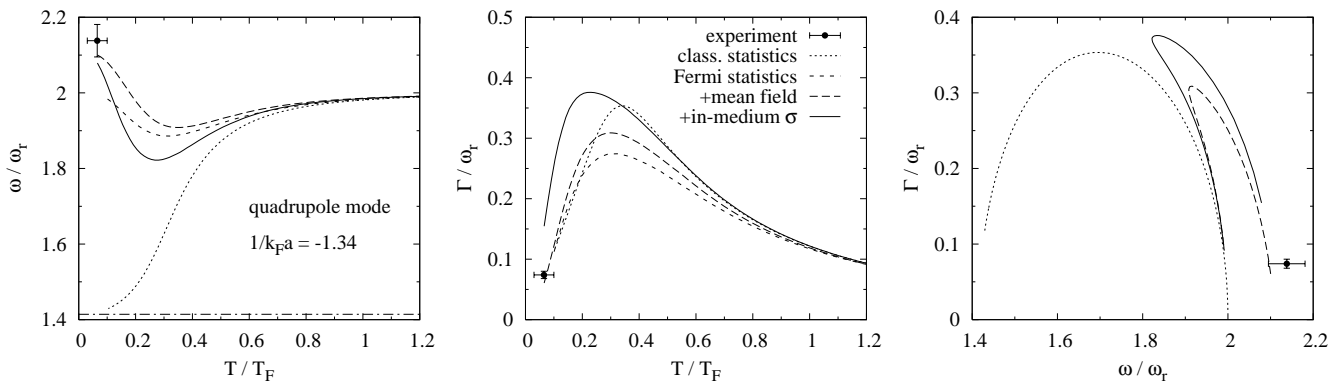


FIG. 4: Frequency and damping of the quadrupole mode for $1/k_F a = -1.34$. The experimental result is taken from Ref. [4]. The three panels display (from left to right) frequency as function of temperature, damping as function of temperature, and damping vs. frequency. The different lines represent different levels of sophistication of the calculation: Starting from a calculation for a classical gas without any mean field and with the scattering cross-section in vacuum (dotted lines), we include the Pauli principle in the equilibrium density profile and in the collision integral (short dashes), then on top of that the mean field U (long dashes), and finally also the in-medium scattering cross section (solid line). The dash-dotted line represents the hydrodynamic frequency, $\omega_{Q,hd} = \sqrt{2}\omega_r$.

U_{eq} and δU terms are included in the Boltzmann equation (36). We still keep the free scattering cross section. Our calculation is limited to temperatures above $0.06T_F$, corresponding to the critical temperature of the system. The mean field does not have a dramatic effect on the damping, but it increases the frequency, especially at low temperature. Frequency and damping at the lowest temperature are now both in excellent agreement with the measured values. Note that the inclusion of the mean field modifies qualitatively the curve Γ vs. ω shown in the third panel of Fig. 4.

Finally, we replace the free scattering cross section by the in-medium one, Eq. (27) (solid lines). Unfortunately, the good agreement between the theoretical results and the measured frequency and damping at low temperature is deteriorated: The resulting damping is too high by a factor of two and the frequency gets shifted downwards, although not dramatically. However, as already mentioned, the calculation is limited to temperatures above $\sim 0.06T_F$ (the critical temperature T_C), while it is possible that the temperature in the experiment was lower (the presence of a small superfluid region in the center of the trap would not contradict the observation of the collisionless frequency [11]). Extrapolating the damping curve obtained with the in-medium cross section to lower temperatures, it seems that the result obtained with in-medium cross section is not necessarily inconsistent with the experiment. Additional experimental data points at higher (and known) temperatures could help to settle this question.

B. Scissors mode at $1/k_F a = -0.45$

Shortly after the quadrupole mode, the Innsbruck group studied the scissors mode at $1/k_F a = -0.45$ and

at unitarity ($1/k_F a = 0$) [5]. In this experiment, the trap had frequencies $\omega_x = 2\pi \times 830$ Hz, $\omega_y = 2\pi \times 415$ Hz, and $\omega_z = 2\pi \times 22$ Hz, and contained $N = 400000$ ^6Li atoms. The frequency ω and damping Γ were measured for constant interaction strength as functions of the temperature. The experimental data for the case $1/k_F a = -0.45$, taken from Ref. [5], are shown in Fig. 5 together with various theoretical results. As in Fig. 4, we display, in addition to ω and Γ as functions of the temperature, Γ as a function of ω .

The meaning of the different curves is the same as in the case of the quadrupole mode discussed in Sec. IV A. The most curious result, which has already been observed in Ref. [17] for the case $1/k_F a = 0$, is that already with classical statistics (dotted line) one can reproduce quite well the observed frequencies: At low temperature, the frequency is the hydrodynamic one ($\sqrt{\omega_x^2 + \omega_y^2} = 2\pi \times 928$ Hz), and with increasing temperature it rises towards the collisionless frequency ($\omega_x + \omega_y = 2\pi \times 1245$ Hz). What is most surprising is that the agreement is very good at temperatures well below the degeneracy temperature T_F , where the classical approximation is not justified at all, while it fails at higher temperatures. In fact, the high-temperature behavior of the frequency is not reproduced by any of the theoretical calculations, which might be due to the importance of the anharmonicity of the trap at high temperatures. The agreement between the measured frequencies and those of a classical gas is, however, purely accidental, as one can see by looking at the corresponding damping rates. The classical statistics leads to a damping which is much too weak at low temperatures (dotted line).

In fact, as in the case of the quadrupole mode discussed in Sec. IV A, the lack of Pauli blocking results in a high collision rate, leading to a perfectly hydrodynamic behavior. The inclusion of Pauli blocking (short

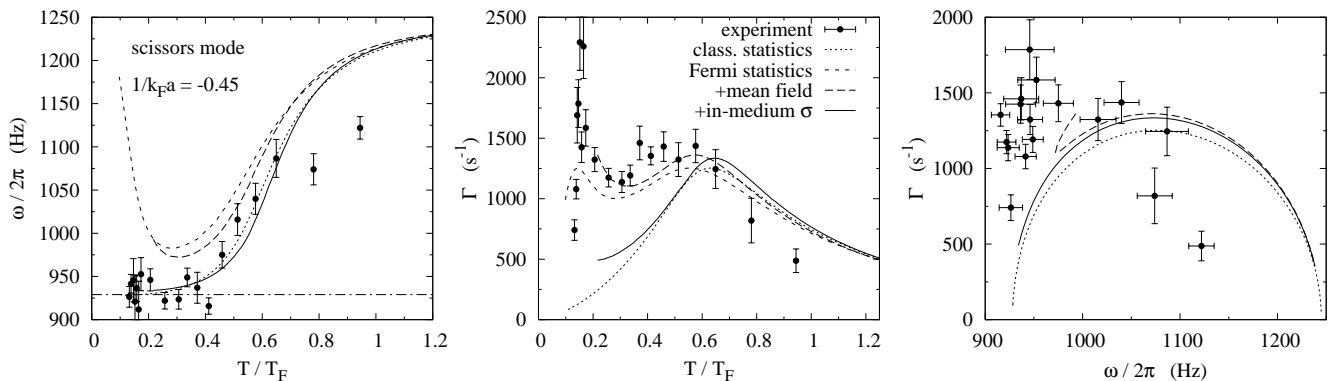


FIG. 5: Same as Fig. 4, but for the scissors mode and $1/k_F a = -0.45$. The data are from Ref. [5]. The dash-dotted line represents the hydrodynamic frequency, $\omega_{S,hd} = \sqrt{\omega_x^2 + \omega_y^2}$

dashes) strongly reduces the collision rate and therefore increases the damping at low temperatures, resulting in a very good agreement with the measured damping rates (except near the peak at $T/T_F \sim 0.15$, which is probably due to the superfluid-normal phase transition). Note that, since the interaction is much stronger now than in the case of the quadrupole mode discussed above, the collisionless regime is not reached, although at low temperature the frequency increases strongly towards the collisionless one. This increase of the frequency is not observed in the experiment, because at these temperatures the system is already in the superfluid phase and therefore its frequency stays close to the hydrodynamic one, even if the collision rate is low. This effect cannot be described in the framework of the simple Boltzmann equation which does not include superfluidity. But also at higher temperatures, the agreement of the frequencies obtained with Fermi statistics (short dashes) with the data is not as good as that obtained with Boltzmann statistics (dotted line).

The inclusion of the mean field (long dashes) leads to a small reduction of the frequency, while the damping is slightly enhanced, improving the agreement with the data. Since our calculation is limited to the normal phase, the curves are restricted to temperatures above $\sim 0.2T_F$ (the critical temperature T_C). The frequencies are now well reproduced for temperatures above $\sim 0.3T_F$, while they are still slightly too high between ~ 0.2 and $\sim 0.3T_F$. The damping is in excellent agreement with the data for all temperatures above T_C .

Finally, the inclusion of the in-medium cross section (solid lines) leads to a big disappointment: The agreement with the data, in particular for the damping, is completely lost. The results are very close to those of the classical gas, similar to the findings of Ref. [26] for the shear viscosity of the unitary gas and of Ref. [6] for different collective modes at unitarity. The reason is that the enhancement of the cross section (cf. Fig. 2) cancels the effect of Pauli blocking.

Apparently the present theory has a fundamental problem. Maybe the quasiparticle approximation made in

Sec. II C is too crude (although the QP density profile coincides very well with the NSR one): There might be important corrections due to energy and momentum dependence of the self-energy [30]. Even the validity of the Boltzmann equation itself might be questioned: The T matrix approximation can result in a long correlation time, leading to non-Markovian (memory) effects [35].

C. Collective modes in the unitary limit

In this subsection we will finally show results for collective modes in the unitary limit ($1/k_F a = 0$). We will again compare with experimental results obtained by the Innsbruck group, Ref. [5] for the case of the scissors mode and Ref. [6] for the radial quadrupole and breathing modes. In the experiment on the scissors mode, the trap parameters were the same as those stated in the beginning of Sec. IV B. Our theoretical results and the experimental data are shown in the first row of Fig. 6, the representations are analogous to those in Figs. 4 and 5.

The quadrupole mode was studied in an axially symmetric trap having $\omega_r = 2\pi \times 1100$ Hz, $\omega_z = 2\pi \times 26$ Hz and containing $N = 600000$ ^6Li atoms [6]. The theoretical results and the experimental data are shown in the second row of Fig. 6. For the radial breathing mode, the trap frequencies were somewhat higher, namely $\omega_r = 2\pi \times 1800$ Hz, $\omega_z = 2\pi \times 32$ Hz, but the number of atoms was again $N = 600000$ [6]. The corresponding theoretical results and experimental data are displayed in the third row of Fig. 6.

In the case of the scissors mode (upper row of Fig. 6), the qualitative features of frequencies and damping as functions of temperature are reasonably well reproduced by all approximations [even by the classical gas (dotted lines), as it happened already in Sec. IV B]. As in the case of the scissors mode at $1/k_F a = -0.45$ discussed in Sec. IV B, the data stay near the hydrodynamic frequency at low temperature because of superfluidity, which is not included in our theory. For temperatures above T_C , which

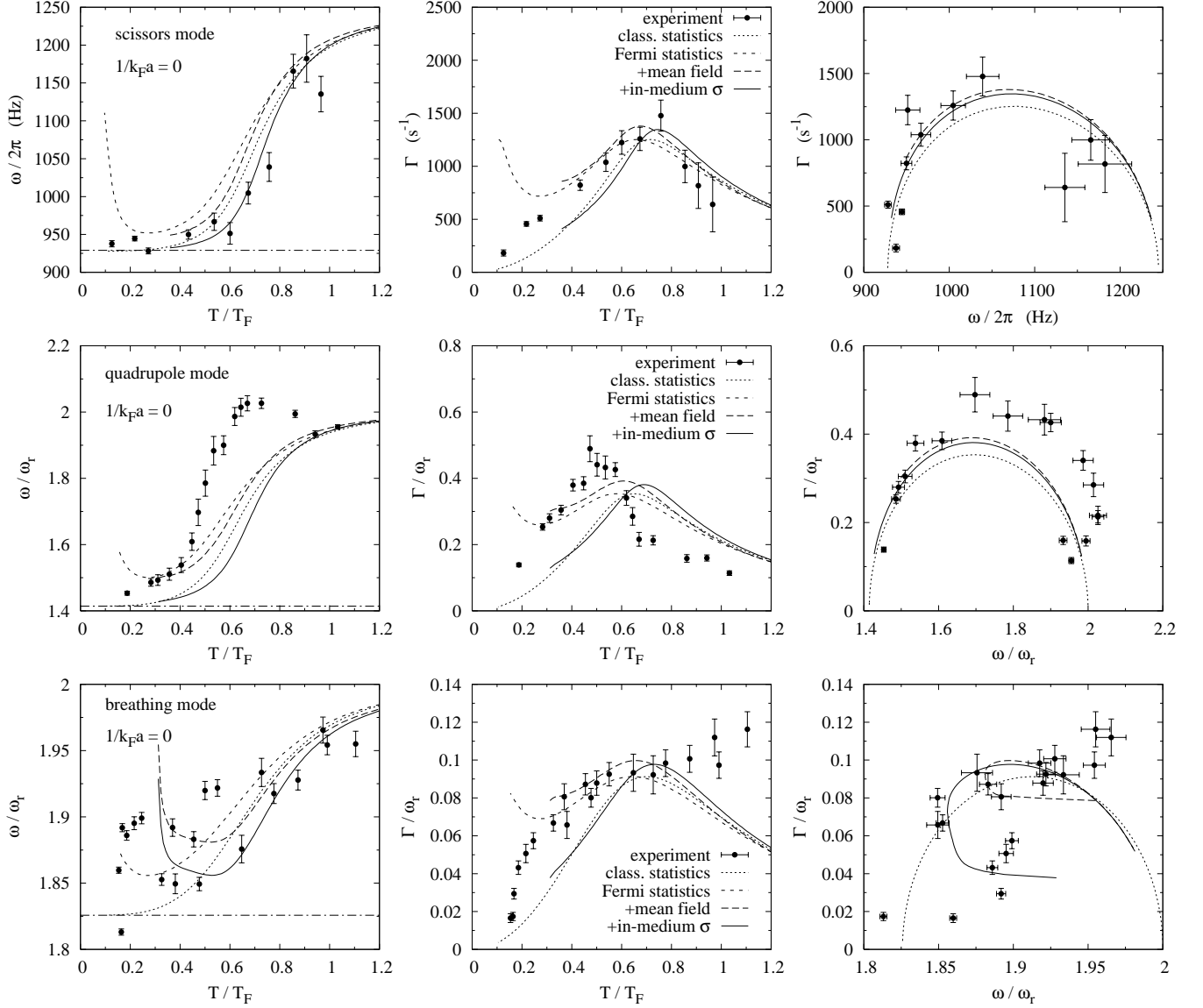


FIG. 6: Same as Fig. 4, but for the scissors mode, the radial quadrupole mode, and the radial breathing mode (from top to bottom) in the unitary limit ($1/k_F a = 0$). The experimental data are taken from Ref. [5] for the scissors mode and from Ref. [6] for the radial quadrupole and breathing modes. The dash-dotted lines represent the respective hydrodynamic frequencies of each mode.

within our theory is given by $T_C \approx 0.3T_F$, the frequencies are best reproduced by the calculation including mean field and in-medium cross section (solid line). Unfortunately, as it happened already in the case $1/k_F a = -0.45$, the strong enhancement of the in-medium cross section leads to a damping which is much smaller than the experimentally observed one. The damping as a function of temperature is best reproduced by the calculation including the mean field but using only the free cross-section in the collision term (long dashes). However, if one looks at the plot Γ vs. ω , both approximations result in curves which are close to the data. This means that both approximations might be compatible with the data, if it turned out that the temperature axis was incorrect.

In this context it should be mentioned that the temperature measurement in the experiment is not evident and in addition not completely independent of the theoretical model used in the analysis. For instance, in the analysis of Ref. [5], the method introduced by Thomas et al. in Ref. [36] was used, which requires, among other things, the knowledge of a parameter β determining the “effective mass” in the unitary limit. As a consequence, in addition to the statistical error in the determination of the temperature, there could be a sizable systematic error coming from theoretical uncertainties. This observation underlines the usefulness of the representation of Γ vs. ω , which is independent of the temperature.

Let us now look at the radial quadrupole mode (sec-

ond row of Fig. 6). In this case, we have to admit that the differences between the different approximations are much smaller than their deviation from the experimental data, i.e., all approximations fail to give a satisfactory description of the data. The mean field has only a very small effect (difference between short and long dashes), and the in-medium cross section (solid line) leads to an additional deterioration as compared to the free one (long dashes). It seems as if in the experiment the continuous transition from the hydrodynamic to the collisionless case happened at a much lower temperature than in any of the theoretical results. But also in the $\omega - \Gamma$ plot, where the experimental data follow a very well defined curve, the theoretical results are quite far from the data. Further studies within an improved theoretical framework are needed.

Concerning the radial breathing mode (third row of Fig. 6), it is difficult to draw firm conclusions from the figures. As it was the case for the scissors mode, the results obtained with mean field but without in-medium cross section (long dashes) give a satisfactory description of the damping between $T_C \approx 0.3T_F$ and $\sim 0.8T_F$, while the damping obtained with the in-medium cross section (solid line) is too weak. Because of their strong scattering, the frequency data seem to be compatible with any of the theoretical curves, except for the sudden rise of the frequencies obtained with mean field (long dashes and solid line) if one approaches T_C from above. This rise of the theoretical frequencies does not come from a reduced collision rate, leading to collisionless behavior, but from a sudden increase of the interaction-dependent parameter χ' (defined in Appendix D). This effect is an artefact of our QP approximation since it occurs when the density profile gets flat at some point different from $\mathbf{r} = 0$, which happens only with the QP densities close to T_C , but not with the NSR densities.

V. CONCLUSIONS

In this paper, we studied the collective modes of a cold Fermi gas with attractive interaction in the framework of the Boltzmann equation with in-medium effects. Our starting point was the T matrix approximation (ladder resummation), which is known to give a satisfactory description of the BCS-BEC crossover. We discussed the corresponding single-particle self energy and in-medium scattering cross section above the critical temperature T_C . Within the QP approximation, which we have to make in view of the Boltzmann equation, the self-energy acts effectively like an attractive mean field, but it avoids the pathological problems of the Hartree approximation. Although we used at the present stage the simplest possible version of the QP approximation (neglecting energy and momentum dependence of the self-energy), it reproduces well the equilibrium density profiles obtained with the NSR formula, except near unitarity close to T_C . The in-medium scattering cross section, which is also obtained

from the T matrix, is strongly enhanced as compared with the free one at low temperature. This is a precursor effect of the transition to the superfluid phase.

We derived the frequencies and damping rates of different collective modes (sloshing, scissors, radial quadrupole, and breathing modes) with inclusion of the “mean field” and in-medium cross section. To that end, we linearized the Boltzmann equation around equilibrium. A first important result is that the frequency of the sloshing mode is equal to the trap frequency even in the presence of the medium effects, in accordance with the Kohn theorem. We stress that this result can only be obtained if one uses in the linearized Boltzmann equation the same mean field as in the calculation of the equilibrium density profile. [It therefore seems dangerous to calculate the sloshing-mode frequency by inserting an interacting density profile (e.g., a measured one), into an equation like Eq. (B2) of Ref. [6] derived from the Boltzmann equation of a non-interacting gas.]

The frequencies and damping rates of the different collective modes were evaluated numerically as functions of the temperature and for different values of the scattering length (parameter $1/k_F a$). Because of the experimental uncertainty concerning the temperature, we discussed in addition the “hydrodynamic circles”, i.e., the damping as a function of the frequency. It was shown that using classical statistics one clearly cannot reproduce the observed collisionless behavior of the modes at small temperatures. By the inclusion of Fermi statistics (Pauli blocking), this problem is solved. Including the mean field on top of Fermi statistics, which is the main topic of this paper, has only a relatively small effect, but nevertheless it leads to a significant improvement of the measured frequencies and damping rates. For instance, we can for the first time quantitatively explain the observed upwards shift of the quadrupole mode in the collisionless normal phase at weak coupling ($1/k_F a = -1.34$), which has attracted a lot of attention. However, in the strongly interacting cases, in particular in the unitary limit, the frequencies depend much more strongly on the collision rate than on the mean field and the mean field effects are of minor importance.

On top of that, we included the in-medium effects in the cross section, which determines the collision rate (relaxation time). Since the in-medium cross section becomes very large when one approaches the critical temperature, this compensates the effect of Pauli blocking and reduces the result of the full calculation to something comparable with the result obtained for a classical gas, as already noted in Refs. [6, 26]. Clearly, this is an up to now unsolved problem and needs further examination. A first possible extension of the present theory is to take into account the energy and momentum dependence of the self-energy in a more involved QP approximation [30].

In addition, the method of taking moments of the Boltzmann equation, although it proved very successful in the past, does not correspond to a full solution of the

Boltzmann equation. In particular, this method is insufficient for a description of the damping due to the anharmonicity of the potential (trap and mean field). In order to improve the calculation in this respect, a more involved numerical method for solving the Boltzmann equation is necessary. A very common method is that using so-called “test-particles”; in the context of trapped fermionic atoms it was used, e.g., in Refs. [14, 15].

Finally, a shortcoming of our present calculation is its limitation to temperatures above T_C , whereas the most interesting experimental results (e.g., extremely strong damping at a certain temperature) are probably related to the transition to the superfluid phase. At least in the weakly coupled regime, it should be possible to include the effects of superfluidity following the approach of Refs. [9, 10]. Work in these directions is in progress.

Acknowledgments

We are grateful to E.R. Sánchez Guajardo for providing us the data of Ref. [5] with the corresponding temperature ratios T/T_F . One of the authors (S.C.) acknowledges financial support provided by Fondazione “A.Della Riccia”.

APPENDIX A: VIRIAL THEOREM

Let us derive a relationship between equilibrium quantities which is very useful for reducing the number of interaction dependent parameters in the explicit expressions for the collective-mode frequencies.

From the Boltzmann equation in equilibrium one obtains the following property of the equilibrium distribution function:

$$\left(\frac{\mathbf{p}}{m} \cdot \nabla_{\mathbf{r}} - \nabla_{\mathbf{r}}(V_T + U_{eq}) \cdot \nabla_{\mathbf{p}}\right) f_{eq}(1 - Af_{eq}) = 0. \quad (\text{A1})$$

Notice that this property was already used in order to derive Eq. (36).

In Ref. [16], where the case $U = g\rho$ is considered for the mean field, it is shown that multiplying equation (A1) by $xp_x^2p_y^2$ and integrating over \mathbf{r} and \mathbf{p} , one obtains the virial theorem $E_{kin} - E_{pot} + 3E_{int}/2 = 0$ [37, 38], with

$$E_{kin} = 2 \int d^3r d^3p \frac{p^2}{2m} f_{eq}, \quad (\text{A2})$$

$$E_{pot} = 2 \int d^3r V_T \rho_{eq}, \quad \text{and} \quad (\text{A3})$$

$$E_{int} = g \int d^3r \rho_{eq}^2. \quad (\text{A4})$$

Here we want to show that the same can be done for any function $U_{eq}(\mathbf{r}) = U[\mu(\mathbf{r}), T]$ in order to obtain a generalized virial theorem.

As mentioned in the end of Sec. II F, we define the rescaled coordinates $\tilde{r}_i = r_i \omega_i / \bar{\omega}$, in terms of which the

trap potential reduces to $V_T = m\bar{\omega}^2 \tilde{r}^2 / 2$, and, consequently, also the density ρ_{eq} and the mean field U_{eq} become spherically symmetric in these coordinates.

It is then found that the generalized virial theorem is

$$E_{kin} - E_{pot} - \int d^3\tilde{r} \rho_{eq} \tilde{r} \frac{\partial U_{eq}}{\partial \tilde{r}} = 0. \quad (\text{A5})$$

In the case $U_{eq} = g\rho_{eq}$ (Hartree approximation), the last term can be integrated by parts, and the well-known result for the virial theorem is recovered.

In the general case, let us define the parameter χ characterizing the strength of the interaction as

$$\chi = -\frac{1}{E_{pot}} \int d^3\tilde{r} \rho_{eq} \tilde{r} \frac{\partial U_{eq}}{\partial \tilde{r}}. \quad (\text{A6})$$

Then the virial theorem can be written as

$$\frac{E_{kin}}{E_{pot}} = 1 - \chi. \quad (\text{A7})$$

APPENDIX B: COMPUTATION OF THE RELAXATION TIME

The equation determining the frequencies of the scissors mode contains the parameter τ , defined in Eq. (50)). Its evaluation is quite involved and we follow closely Ref. [39] in order to reduce the number of integrals. The integral I_S entering the definition of τ can be most conveniently computed if one observes that

$$I_S = \frac{1}{10} \sum_{ij} I_{ijij}. \quad (\text{B1})$$

The explicit expression for I_S reads now

$$I_S = \frac{1}{10} \int d^3r d^3p d^3p_1 d\Omega \frac{d\sigma}{d\Omega} \frac{|\mathbf{p} - \mathbf{p}_1|}{m} \times f_{eq} f_{eq1} (1 - Af'_{eq})(1 - Af'_{eq1}) \times [p^4 + (\mathbf{p} \cdot \mathbf{p}_1)^2 - (\mathbf{p} \cdot \mathbf{p}')^2 - (\mathbf{p} \cdot \mathbf{p}'_1)^2]. \quad (\text{B2})$$

In order to reduce the number of integrals, one first introduces the variables $\mathbf{k} = \mathbf{p} + \mathbf{p}_1$, $\mathbf{q} = (\mathbf{p} - \mathbf{p}_1)/2$, and $\mathbf{q}' = (\mathbf{p}' - \mathbf{p}')/2$ (remember that $|\mathbf{q}| = |\mathbf{q}'|$). In terms of these variables, the factor in the second line of Eq. (B2) becomes

$$\frac{1}{4A^2} \frac{1}{\cosh \beta(E - \mu_0) + \cosh \beta \mathbf{k} \cdot \mathbf{q}/2m} \times \frac{1}{\cosh \beta(E - \mu_0) + \cosh \beta \mathbf{k} \cdot \mathbf{q}'/2m}, \quad (\text{B3})$$

with $E = k^2/4m + q^2/2m + V_T + U$. The factor in the third line of Eq. (B2) reduces to $2q^4 - 2(\mathbf{q} \cdot \mathbf{q}')^2 + (\mathbf{k} \cdot \mathbf{q})^2/2 - (\mathbf{k} \cdot \mathbf{q}')^2/2$. Note that the last two terms do not contribute to the integral since they are antisymmetric with respect to the interchange $\mathbf{q} \leftrightarrow \mathbf{q}'$. Let us now

denote by θ, ϕ and θ', ϕ' the zenith and azimuth angles of \mathbf{q} and \mathbf{q}' , respectively, with respect to \mathbf{k} . The integrals over ϕ and ϕ' , which appear only in the third line of Eq. (B2), can be done analytically and, writing $\gamma = \cos \theta$ and $\gamma' = \cos \theta'$, we are finally left with

$$I_S = \frac{1}{20\pi^2 m} \int_0^\infty d\tilde{r} \tilde{r}^2 \int_0^\infty dk k^2 \int_0^\infty dq q^7 \frac{d\sigma}{d\Omega} \times \int_{-1}^1 d\gamma \int_{-1}^1 d\gamma' (1 + 2\gamma^2 - 3\gamma^2 \gamma'^2) \times \frac{1}{\cosh \beta(E - \mu_0) + \cosh \beta k q \gamma / 2m} \times \frac{1}{\cosh \beta(E - \mu_0) + \cosh \beta k q \gamma' / 2m}. \quad (\text{B4})$$

This five-dimensional integral is evaluated numerically using a Monte-Carlo algorithm.

APPENDIX C: FREQUENCIES OF THE SCISSORS MODE

In order to determine the frequency of the collective modes, one has to take moments of the Boltzmann equation. It is thus useful to rewrite Eq. (36)) as

$$f_{eq}(1 - Af_{eq})\dot{\Phi} - (\nabla_p f_{eq}) \cdot \nabla_r (T\Phi + \frac{dU_{eq}}{d\rho_{eq}} \delta\rho) + T(\nabla_r f_{eq}) \cdot \nabla_p \Phi = -I[\Phi], \quad (\text{C1})$$

and to denote the three terms on the lhs by (i), (ii), and (iii). When integrating over \mathbf{r} and \mathbf{p} , the following identities are useful:

$$\nabla_p f_{eq} = -\frac{\beta}{m} f_{eq}(1 - Af_{eq})\mathbf{p}, \quad (\text{C2})$$

$$\frac{\partial f_{eq}}{\partial \mu} = \beta f_{eq}(1 - Af_{eq}) \left(1 - \frac{\partial U_{eq}}{\partial \mu} \Big|_T\right), \quad (\text{C3})$$

$$\frac{\partial}{\partial \mu} \dots \Big|_T = -\frac{1}{m\bar{\omega}^2 \tilde{r}} \frac{\partial}{\partial \tilde{r}} \dots \quad (\text{C4})$$

As an example, we report in more detail the derivation of the modified frequencies of the scissors mode. The corresponding trial function Φ is given in Table I.

The contributions of the term (i) to the moments of Boltzmann equation are:

$$\int d^3 r d^3 p (i) xy = -\frac{i\omega E_{pot}(1 + \varphi_1)}{3\beta m^2 \omega_x^2 \omega_y^2} e^{-i\omega t} c_1, \quad (\text{C5})$$

$$\int d^3 r d^3 p (i) xp_y = -\frac{i\omega E_{pot}}{3\beta \omega_x^2} e^{-i\omega t} c_2, \quad (\text{C6})$$

$$\int d^3 r d^3 p (i) yp_x = -\frac{i\omega E_{pot}}{3\beta \omega_y^2} e^{-i\omega t} c_3, \quad (\text{C7})$$

$$\int d^3 r d^3 p (i) p_x p_y = -\frac{i\omega m^2 E_{kin}}{3\beta} e^{-i\omega t} c_4, \quad (\text{C8})$$

where the parameter φ_1 is defined as

$$\varphi_1 = \frac{1}{5E_{pot}} \int d^3 \tilde{r} \tilde{r}^2 \frac{\partial \rho_{eq}}{\partial \tilde{r}} \frac{\partial U_{eq}}{\partial \tilde{r}} \frac{1}{1 + \frac{1}{m\bar{\omega}^2 \tilde{r}} \frac{\partial U_{eq}}{\partial \tilde{r}}}. \quad (\text{C9})$$

The density variation is given by

$$\delta\rho = e^{-i\omega t} c_1 xy \frac{1}{\beta} \frac{\partial \rho_{eq}}{\partial \mu} \frac{1}{1 - \frac{\partial U_{eq}}{\partial \mu}}. \quad (\text{C10})$$

Using this, we can write for the contributions of (ii) to the moments of the Boltzmann equation:

$$\int d^3 r d^3 p (ii) xy = 0, \quad (\text{C11})$$

$$\int d^3 r d^3 p (ii) xp_y = \frac{(1 + \varphi_1)E_{pot}}{3\beta m \omega_x^2} e^{-i\omega t} c_1, \quad (\text{C12})$$

$$\int d^3 r d^3 p (ii) yp_x = \frac{(1 + \varphi_1)E_{pot}}{3\beta m \omega_y^2} e^{-i\omega t} c_1, \quad (\text{C13})$$

$$\int d^3 r d^3 p (ii) p_x p_y = \frac{mE_{kin}}{\beta} e^{-i\omega t} (c_2 + c_3). \quad (\text{C14})$$

Finally, the (iii) contributions to the moments of Boltzmann equation are:

$$\int d^3 r d^3 p (iii) xy = -\frac{E_{pot}}{3\beta m} e^{-i\omega t} \left(\frac{c_3}{\omega_y^2} + \frac{c_2}{\omega_x^2}\right), \quad (\text{C15})$$

$$\int d^3 r d^3 p (iii) xp_y = -\frac{mE_{kin}}{3\beta} e^{-i\omega t} c_4, \quad (\text{C16})$$

$$\int d^3 r d^3 p (iii) yp_x = -\frac{mE_{kin}}{3\beta} e^{-i\omega t} c_4, \quad (\text{C17})$$

$$\int d^3 r d^3 p (iii) p_x p_y = 0. \quad (\text{C18})$$

With these results, the equations for the coefficients c_i read

$$\begin{aligned} i\omega(1 + \varphi_1)c_1 + m\omega_y^2 c_2 + m\omega_x^2 c_3 &= 0, \\ (1 + \varphi_1)c_1 - im\omega c_2 - (1 - \chi)m^2 \omega_x^2 c_4 &= 0, \\ (1 + \varphi_1)c_1 - im\omega c_3 - (1 - \chi)m^2 \omega_y^2 c_4 &= 0, \\ c_2 + c_3 + m\left(\frac{1}{\tau} - i\omega\right)c_4 &= 0. \end{aligned} \quad (\text{C19})$$

The system has a solution if

$$\begin{aligned} \frac{i\omega}{\tau} [\omega^2 - (\omega_x^2 + \omega_y^2)] + \omega^4 - 2\omega^2(\omega_x^2 + \omega_y^2)(1 - \chi/2) \\ + (\omega_x^2 - \omega_y^2)^2 (1 - \chi) &= 0, \end{aligned} \quad (\text{C20})$$

which is Eq. (51) with $\omega_{S,hd}$ and $\omega_{S,cl}$ given by Eqs. (52) and (53).

APPENDIX D: FREQUENCIES OF THE BREATHING MODES

We consider a trap with frequencies $\omega_x = \omega_y = \omega_r$ and $\omega_z = \lambda\omega_r$.

	$x^2 + y^2$	z^2	$xp_x + yp_y$	zp_z	$p_x^2 + p_y^2$	p_z^2
$x^2 + y^2$	$\frac{2i\omega(1+\varphi_1)}{m^2\omega_r^2}$	$\frac{i\omega(1+\varphi_1)}{2m^2\omega_r^2}$	$\frac{1}{m}$	0	$i\omega$	$\frac{i\omega}{2}$
z^2	$\frac{2i\omega(1+\varphi_1)}{m^2\omega_r^2}$	$\frac{3i\omega(1+\varphi_1)}{m^2\omega_r^2}$	0	$\frac{2}{m}$	$2i\omega$	$i\omega$
$xp_x + yp_y$	$\frac{2(1+2\varphi_1-\varphi_3)}{m}$	$\frac{\varphi_1-\varphi_3}{m}$	$-i\omega$	0	$-2m\omega_r^2(1-2\chi+2\chi')$	$m\omega_r^2(\chi-2\chi')$
zp_z	$\frac{2(\varphi_1-\varphi_3)}{m}$	$\frac{2+3\varphi_1-\varphi_3}{m}$	0	$\frac{-i\omega}{\lambda^2}$	$2m\omega_r^2(\chi-2\chi')$	$-2m\omega_r^2(1-\frac{3}{2}\chi+\chi')$
$p_x^2 + p_y^2$	$\frac{i\omega}{m^2\omega_r^2(1-\chi)}$	$\frac{i\omega}{2m^2\omega_r^2(1-\chi)}$	$-\frac{1}{m}$	0	$2i\omega - \frac{1}{3\tau}$	$\frac{i\omega}{2} + \frac{1}{3\tau}$
p_z^2	$\frac{i\omega}{m^2\omega_r^2(1-\chi)}$	$\frac{i\omega}{2m^2\omega_r^2(1-\chi)}$	0	$-\frac{1}{m}$	$i\omega + \frac{2}{3\tau}$	$\frac{3}{2}i\omega - \frac{2}{3\tau}$

In Table D, each line is obtained by taking one moment of the Boltzmann equation. For example, the third entry in the first column ($1/m$) is the coefficient in front of c_3 if Eq. (C1), with Φ as given in the last line of Table I, is multiplied by $x^2 + y^2$ and integrated over \mathbf{r} and \mathbf{p} . Notice that the coefficient λ appears only through the zp_z term. The new interaction dependent parameters χ' and φ_3 that enter in the table are defined as:

$$\chi' = \frac{3}{2E_{pot}} \int d^3\tilde{r} \rho_{eq}^2 \frac{\partial U_{eq}}{\partial \rho_{eq}}, \quad (D1)$$

$$\varphi_3 = -\frac{1}{E_{pot}} \int d^3\tilde{r} \tilde{r} \rho_{eq} \frac{\partial U_{eq}}{\partial \tilde{r}} \frac{1}{1 + \frac{1}{m\bar{\omega}^2\tilde{r}} \frac{\partial U_{eq}}{\partial \tilde{r}}}. \quad (D2)$$

where χ' reduces to $3E_{int}/2E_{pot}$ in the Hartree case. From the determinant of the 6×6 matrix given in Table D, we obtain the equation for the frequencies, Eq. (57). The frequencies in the collisionless limit are given by

$$\omega_{B,cl\pm}^2 = \omega_r^2 \frac{a \pm \sqrt{a^2 + b}}{16 + 25\varphi_1 - 25\chi(1 + \varphi_1)} \quad (D3)$$

with

$$a = 25\chi^2(1 + \lambda^2)(1 + \varphi_1) + 2[\chi'(2 + \lambda^2)(8 + 5\varphi_1) + (1 + \lambda^2)(16 + 25\varphi_1) - 4(2 + \lambda^2)\varphi_3] + \chi[-10\chi'(2 + \lambda^2)(1 + \varphi_1) - 3(1 + \lambda^2)(22 + 25\varphi_1) + 8(2 + \lambda^2)\varphi_3], \quad (D4)$$

$$b = -4\lambda^2(2 - \chi)[16 + 25\varphi_1 - 25\chi(1 + \varphi_1)] \times [32 + 50\varphi_1 + 25\chi^2(1 + \varphi_1) + 6\chi'(8 + 5\varphi_1) - 3\chi(22 + 25\varphi_1 + 10\chi'(1 + \varphi_1) - 8\varphi_3) - 24\varphi_3], \quad (D5)$$

The hydrodynamic frequencies are

$$\omega_{B,hd\pm}^2 = \omega_r^2 \frac{c \pm \sqrt{c^2 + d}}{3[16 + 25\varphi_1 - 25\chi(1 + \varphi_1)]}, \quad (D6)$$

with

$$c = 25\chi^2(2 + \lambda^2)(1 + \varphi_1) + 6\chi'(2 + \lambda^2)(8 + 5\varphi_1) + (5 + 4\lambda^2)(16 + 25\varphi_1) - 24(2 + \lambda^2)^2\varphi_3 + \chi[-157 - 175\varphi_1 - 30\chi'(2 + \lambda^2)(1 + \varphi_1) + 48\varphi_3 + \lambda^2(-116 - 125\varphi_1 + 24\varphi_3)], \quad (D7)$$

$$d = -36\lambda^2[16 + 25\varphi_1 - 25\chi(1 + \varphi_1)] \times [32 + 50\varphi_1 + 25\chi^2(1 + \varphi_1) + 6\chi'(8 + 5\varphi_1) - 3\chi(22 + 25\varphi_1 + 10\chi'(1 + \varphi_1) - 8\varphi_3) - 24\varphi_3], \quad (D8)$$

Note that since b and d are proportional to λ , the low-lying limiting frequencies ($\omega_{B,cl-}^2$ and $\omega_{B,hd-}^2$), corresponding to the axial breathing mode, tend to zero in the limit of a very elongated trap ($\lambda \rightarrow 0$).

In absence of the mean field, $\chi = \chi' = \varphi_1 = \varphi_3 = 0$ and the frequencies reduce to the known expressions [12, 16]

$$\omega_{B,cl\pm}^2 = 2\omega_r^2(1 + \lambda^2 \pm \sqrt{1 - 2\lambda^2 + \lambda^4}), \quad (D9)$$

$$\omega_{B,hd\pm}^2 = \frac{\omega_r^2}{3}(5 + 4\lambda^2 \pm \sqrt{25 + 16\lambda^4 - 32\lambda^2}). \quad (D10)$$

- [1] J. Kinast, S.L. Hemmer, M.E. Gehm, A. Turlapov, and J.E. Thomas, Phys. Rev. Lett. **92**, 150402 (2004).
[2] J. Kinast, A. Turlapov, and J.E. Thomas, Phys. Rev. A **70**, 051401(R) (2004).
[3] M. Bartenstein, A. Altmeyer, S. Riedl, S. Jochim, C.

- Chin, J. Hecker Denschlag, and R. Grimm, Phys. Rev. Lett. **92**, 203201 (2004).
[4] A. Altmeyer, S. Riedl, C. Kohstall, M.J. Wright, R. Geursen, M. Bartenstein, C. Chin, J. Hecker Denschlag, and R. Grimm, Phys. Rev. Lett. **98**, 040401 (2007).

- [5] M.J. Wright, S. Riedl, A. Altmeyer, C. Kohstall, E.R. Sánchez Guajardo, J. Hecker Denschlag, and R. Grimm, Phys. Rev. Lett. **99**, 150403 (2007).
- [6] S. Riedl, E.R. Sánchez Guajardo, C. Kohstall, A. Altmeyer, M.J. Wright, J. Hecker Denschlag, R. Grimm, G.M. Bruun, and H. Smith, Phys. Rev. A **78**, 053609 (2008).
- [7] M. Cozzini and S. Stringari, Phys. Rev. Lett. **91**, 070401 (2003).
- [8] E. Taylor and A. Griffin, Phys. Rev. A **72**, 053630 (2005).
- [9] M. Urban and P. Schuck, Phys. Rev. A **73**, 013621 (2006);
- [10] M. Urban, Phys. Rev. A **75**, 053607 (2007).
- [11] M. Urban, Phys. Rev. A **78**, 053619 (2008).
- [12] C. Menotti, P. Pedri, and S. Stringari, Phys. Rev. Lett. **89**, 250402 (2002).
- [13] P. Pedri, D. Guéry-Odelin, and S. Stringari, Phys. Rev. A **68**, 043608 (2003).
- [14] F. Toschi, P. Vignolo, S. Succi, and M.P. Tosi, Phys. Rev. A **67**, 041605(R) (2003).
- [15] F. Toschi, P. Capuzzi, S. Succi, P. Vignolo, and M.P. Tosi, J. Phys. B **37**, S91 (2004).
- [16] P. Massignan, G.M. Bruun, and H. Smith, Phys. Rev. A **71**, 033607 (2005).
- [17] G.M. Bruun and H. Smith, Phys. Rev. A **76**, 045602 (2007).
- [18] W. Kohn, Phys. Rev. **123**, 1242 (1961).
- [19] L. Brey, N.F. Johnson, and B.I. Halperin, Phys. Rev. B **40**, 10647 (1989).
- [20] M. Houbiers, R. Ferwerda, H.T.C. Stoof, W.I. McAlexander, C.A. Sackett, and R.G. Hulet, Phys. Rev. A **56**, 4864 (1997).
- [21] P. Nozières and S. Schmitt-Rink, J. Low. Temp. Phys. **59**, 195 (1985).
- [22] H. Heiselberg, Phys. Rev. A **63**, 043606 (2001).
- [23] A.L. Fetter and J.D. Walecka, *Quantum Theory of Many-Particle Systems* (McGraw-Hill, New York, 1971).
- [24] P. Pieri and G.C. Strinati, Phys. Rev. B **61**, 15 370 (2000).
- [25] A. Perali, P. Pieri, G.C. Strinati, and C. Castellani, Phys. Rev. B **66**, 024510 (2002).
- [26] G.M. Bruun and H. Smith, Phys. Rev. A **75**, 043612 (2007).
- [27] C.A.R. Sá de Melo, M. Randeria, and J.R. Engelbrecht, Phys. Rev. Lett. **71**, 3202 (1993).
- [28] T. Alm, G. Röpke, and M. Schmidt, Phys. Rev. C **50**, 31 (1994); T. Alm, G. Röpke, W. Bauer, F. Daffin, and M. Schmidt, Nucl. Phys. A **587**, 815 (1995).
- [29] A. Perali, P. Pieri, L. Pisani, G.C. Strinati, Phys. Rev. Lett. **92**, 220404 (2004).
- [30] P. Danielewicz, Ann. Phys. (N.Y.) **152**, 239 (1984).
- [31] E.M. Lifshitz and L.P. Pitaevskii, *L.D. Landau and E.M. Lifshitz, Course of Theoretical Physics, Vol. 10: Physical Kinetics* (Pergamon, Oxford, 1981).
- [32] E.M. Lifshitz and L.P. Pitaevskii, *L.D. Landau and E.M. Lifshitz, Course of Theoretical Physics, Vol. 9: Statistical Physics, part 2* (Pergamon, Oxford, 1980).
- [33] U. Al Khawaja, C.J. Pethick, and H. Smith, J. Low Temp. Phys. **118**, 127 (2000).
- [34] M. Bartenstein, A. Altmeyer, S. Riedl, S. Jochim, C. Chin, J. Hecker Denschlag, and R. Grimm, Phys. Rev. Lett. **92**, 203201 (2004).
- [35] D. Kremp, M. Bonitz, W.D. Kraeft, and M. Schlanges, Ann. Phys. (N.Y.) **258**, 320 (1997).
- [36] J. E. Thomas, J. Kinast, and A. Turlapov, Proceedings of the 24th International Conference on Low Temperature Physics, AIP Conf. Proc. **850**, 69 (2006).
- [37] F. Dalfovo, S. Giorgini, L.P. Pitaevskii, and S. Stringari, Rev. Mod. Phys. **71**, 463 (1999).
- [38] L. Vichi and S. Stringari, Phys. Rev. A **60**, 4734 (1999).
- [39] L. Vichi, J. Low Temp. Phys. **121**, 177 (2000).